HHS Public Access

Author manuscript

Biosens Bioelectron. Author manuscript; available in PMC 2017 June 15.

Published in final edited form as:

Biosens Bioelectron. 2016 June 15; 80: 230–236. doi:10.1016/j.bios.2016.01.060.

Electrical response of B cell lines latently infected with Kaposi's sarcoma herpesvirus

Mohammadali Safavieh[1,⊥], **Sultan Khetani**[1,⊥], **Franceline Juillard**[2], **Vivasvat Kaul**[1], **Manoj Kumar Kanakasabapathy**[1], **Kenneth M Kaye**[2], and **Hadi Shafiee**[1]

Hadi Shafiee: hshafiee@research.bwh.harvard.edu

[1]Division of Biomedical Engineering, Division of Renal Medicine, Department of Medicine, Brigham and Women's Hospital, Harvard Medical School, Boston, MA, USA

[2]Department of Medicine, Brigham and Women's Hospital, Harvard Medical School, Boston, MA, USA

Abstract

Certain viruses, such as herpesviruses, are capable of persistent and latent infection of host cells. Distinguishing and separating live, latently infected cells from uninfected cells is not easily attainable using current approaches. The ability to perform such separation would greatly enhance the ability to study primary, infected cells and potentially enable elimination of latently infected cells from the host. Here, the dielectrophoretic response of B cells infected with Kaposi's sarcoma-associated herpesvirus (KSHV) were investigated and compared to uninfected B cells. We evaluated the effect of applied voltage, signal frequency, and flow rate of the sample on the cell capture efficiency. We achieved 37.1%%±8.5% difference in capture efficiencies between latently KSHV-infected and uninfected BJAB cells at the chip operational conditions of 1V, 50 KHz and 0.02 μl/min sample flow rate. Our results show that latently infected B cell lines demonstrated significantly different electrical response compared to uninfected B cells and DEP-based microchips can be potentially used for sorting latently infected cells based on their electrical properties.

Introduction

Certain viruses, including Kaposi's sarcoma-associated herpesvirus (KSHV) and Human Immunodeficiency Virus (HIV) can establish lifetime latent infection in host cells such as B cells or $CD4^+$ T cells. These viral reservoirs persist in infected individuals even after effective treatment. Eradicating such viral infections requires inhibiting viral replication, identifying non-replicating latently infected reservoirs, and eliminating these reservoirs. For example, antiretroviral therapy (ART) cannot completely eradicate HIV as it cannot identify

Correspondence to: Hadi Shafiee, hshafiee@research.bwh.harvard.edu.

⊥Authors with equal contribution

and eliminate latently infected resting memory $CD4^+$ T cells that harbour an integrated HIV genome while they are not producing viral proteins (Chun et al. 1997; Chun et al. 1995; Finzi et al. 1997; Wong et al. 1997). These cellular reservoirs, present in all HIV-infected individuals, are not detectable by the immune system. Therefore, selectively identifying and sorting latently infected cells will open new avenues to investigate these latent reservoirs and could lead to more effective therapies for such viral infections (Finzi et al. 1999).

KSHV is the etiologic agent of Kaposi's sarcoma (KS), an angioproliferative malignancy that can involve the skin or internal organs (Ganem 2006). In addition to KS, KSHV also has a causative role in primary effusion B-cell lymphoma (PEL) (Jones et al. 1998) and multi-centric Castleman's disease (an aggressive lympho-proliferative disorder) (Kikuta et al. 1997; Soulier and et al 1995). These tumors occur most commonly in immunosuppressed individuals, including those with HIV/AIDS, and in patients such as transplant recipients receiving immunosuppressive therapy. KSHV typically establishes latent infection. During latent infection, KSHV genome persists as a multi-copy, circularized, extra chromosomal episome (plasmid). The ~165 kb KSHV genome is comprised of double stranded DNA, and encodes more than 80 viral proteins and non coding RNAs. During latent infection, virions are not produced and only a few viral genes are expressed. B cells are important sites of KSHV latency. One latently infected cell can carry 1 to more than 80 KSHV episomal genomes (Ganem 2007). Latent virus reactivates in a small subset of cells, resulting in the production of infectious virions (Villarreal 2005).

Infection of cells by microorganisms leads to changes in cells' mechanical or biochemical properties, which maybe used as biomarkers for identifying infected cells. For example, *Plasmodium falciparum*-infected red blood cells (RBCs) showed significant differences in its cell deformation, magnetic, and electrical properties compared with uninfected RBCs(Guo et al. 2012; Nam et al. 2013; Soo Hoo et al. 2004). Various platforms have been developed to sort infected RBCs based on their morphological changes. Guo *et al*. developed a microfluidic chip to identify *Plasmodium falciparum*-infected RBCs utilizing its mechanical cell deformation properties (Guo et al. 2012). Using pressure driven flow, it was demonstrated that parasitized RBCs were 1.5 to 200 times stiffer than uninfected RBCs. Alternatively, malaria-infected RBCs were isolated from uninfected cells using unique paramagnetic characteristics of malaria bi-product (hemozoin) within a magnetic gradient field (Nam et al. 2013). In other work, Adenovirus-infected HeLa and 293 cells were separated based on their optophoretic responses in an optophoresis optical gradient field (Soo Hoo et al. 2004). It was observed that the optophoretic motility increased by 12% to 17% in infected Hela cells and 40% in infected 293 cells (Soo Hoo et al. 2004). Hamden *et al*. also showed that KSHV-infected cells demonstrate unique Raman spectrum signature compared to uninfected cells (Hamden et al. 2005; Moor et al. 2014).

Furthermore, biological activities of cells and cellular interactions with external agents such as bacteria and viruses can have a significant effect on cells' electrical properties and polarization (Archer et al. 1999; Gascoyne et al. 1997; Hampl et al. 1981; Krempien et al. 1984; Rixon et al. 1992; Schlehofer et al. 1979). A number of factors can cause variations in the electrical signature of infected cells. For instance, in malaria-infected RBCs, there is a decrease in the net negative charge present in the erythrocyte membrane. Aceti *et al*.

reported that erythrocyte membranes of *Plasmodium falciparum*-infected RBCs demonstrated a higher electrical conductivity within the frequency range of 10 KHz to 100 MHz in bulk suspension (Aceti et al. 1990). This change in conductivity causes a variation in dielectrophoretic response (Gascoyne et al. 1997), which has been observed in other cell types such as leukemia and metastatic breast cancer cells (Becker et al. 1995). Dielectrophoresis (DEP) is the motion of polarized particles in non-uniform electric field and can be used as an effective modality to sort rare cells of interest in biological samples (Pohl and Crane 1971; Salmanzadeh et al. 2012a; Salmanzadeh et al. 2012b; Shafiee et al. 2009; Shafiee et al. 2010). Here, we studied the DEP response of latently KSHV-infected and uninfected BJAB cells in a microfluidic device. We evaluated the effect of sample flow rate, applied voltage and frequency on cell capture and cell capture efficiency for KSHV-infected BJAB and uninfected BJAB cells using a microfluidic device as shown in Fig. 1.

Materials & Method

Cell Culture

BJAB cells were cultured in Roswell Park Memorial Institute (RPMI) medium (Gibco, Life Technologies) containing 10% bovine growth serum (BGS) (HyClone GE Healthcare) and 15 μg/ml gentamicin (Gemini bio-product, California, USA). KSHV-infected BJAB cells (Chen and Lagunoff 2005) were maintained in RPMI medium containing 10% BGS, 15 μg/ml gentamicin, and 17 μg/ml puromycin (InvivoGen, San Diego, California). BJAB cells expressing green fluorescent protein (GFP) from the pEGFP-C1 plasmid, were cultured in RPMI medium containing 10% BGS, 15 μg/ml gentamicin and 800 μg/ml G418 (Gemini bio-product). Three low electrically conductive DEP Buffers were prepared. DEP Buffer I was composed of 8.5% Sucrose (w/v), 0.3% Glucose (w/v), and 0.725% RPMI in DI water. DEP buffer II was composed of 0.0025 g/ml glucose, 0.09 g/ml sucrose, 6 ml of Dulbecco's Modified Eagle Medium (DMEM) (Gibco, life technologies), and 40 ml of DI water. Lastly, DEP buffer III was composed of 135 mg Sucrose, 326mg Dextrose (Sigma Aldrich, MO, USA), and 45 ml of DI water. The conductivity of DEP buffers I, II and III were 100 μS/cm, 1.6 μS/cm and 1μS/cm, respectively. For KSHV-infected BJAB cell lines, we infected BJAB with KSHV recombinant virus carrying an expression cassette for GFP(Chen and Lagunoff 2005).

Cell Capturing Technique

To perform the DEP experiments, infected and uninfected BJAB cells at stock concentration were washed twice with DEP buffers by centrifuging at 250 g for 3 minutes to remove the electrically conductive cell media. The microfluidic chip with interdigitated electrodes was placed on an inverted microscope (Carl Zeiss Axio Observer DI) (Fig. 1A). A 1 ml BD Luer-Lok syringe was filled with the sample containing the mixture of uninfected BJAB and latently KSHV-infected BJAB cells suspended in DEP buffer (Fig. 1B). A needle (Small Parts Inc., Miami, Florida) was attached to the tip of the syringe, which was then connected via tubing to the microfluidic chip. The syringe was then placed into the holding bracket of a syringe pump (New Era Pump System Inc., New York, NY). The diameter settings on the pump were set to 0.8 mm to match the diameter of the tubing. Bright-field mode was used to observe both of the cell populations while GFP mode was set to view the KSHV–infected,

GFP–tagged BJAB cells on the chip. The electrodes on DEP microchip were wired to a HP 8116 pulse/function generator (Hewlett-Packard, California, USA) to modulate the dielectrophoretic forces on cells by varying voltages and frequencies. Capture efficiency was defined as the ratio between captured cells with respect to the total injected cells. The difference between capturing efficiency of KSHV-infected BJAB and uninfected BJAB was defined as Δ(C.E.). To evaluate the effect of frequency on cell capture efficiency, the frequency of the signal was increased from 10 KHz to 100 KHz at a constant flow rate and applied voltage. We also evaluated the cells' DEP response for applied voltages of 0.5 V and 1 V at constant frequency and flow rate. The effect of flow rate on cell capture efficiency was also investigated for 0.01 μl/min, 0.02 μl/min, and 0.03 μl/min flow rates at a constant applied voltage and frequency. Captured cells were observed under microscope and images were taken in bright-field mode.

Fluorescence Microscopy

Cells were spread onto slides and fixed in 4%(v/v) paraformaldehyde (Sigma Aldrich) in 1× phosphate-buffered saline (PBS) (Gibco, Life Technologies) for 10 minutes at room temperature. After three washes with PBS, cells were permeabilized using 0.5% Triton X-100 in 1× PBS for 5 minutes at room temperature. Coverslips were applied using Aqua-Poly Mount (Polysciences, Warrington, PA). Cells were spread onto slides and fixed in 4% (v/v) paraformaldehyde (Sigma Aldrich) in 1× phosphate-buffered saline (PBS) (Gibco, Life Technologies) for 10 minutes at room temperature. After three washes with PBS, cells were permeabilized using 0.5% Triton X-100 in 1× PBS for 5 minutes at room temperature. To detect latency-associated nuclear antigen (LANA), cell spreads were incubated with anti-LANA monoclonal antibody LN53 (1:300; Advanced Biotechnologies), which detects a multicopy epitope located in the LANA repeat region (Fig 1E&F). For the secondary antibody, an Alexa Fluor 568-conjugated anti-rat antibody (1:1,000; Molecular Probes) was used. Cells were counterstained with Hoechst 33258 (Fig. 1C&D) (Invitrogen, Carlsbad, California, USA) at 10 μg/ml and Aqua-Poly/Mount (Polysciences) applied prior to coverslips. Images of stained uninfected and infected B cells were taken using a Zeiss AxioPlan 2 microscope (Thornwood, NY) at a magnification of 630× (Fig. 1C–H).

Microchip Fabrication

Interdigitated gold electrodes were fabricated on a Pyrex glass substrate using E-beam lithography (Donthu et al. 2005; Tseng et al. 2003; Vieu et al. 2000) and lift-off technique (Jokerst et al. 1995) with a width and spacing of 10 μm. The microchannels (7 mm in length and 2 mm in width) were first cut on 50 μm thick double-sided adhesives (DSA) using a laser cutter (Universal laser systems, AZ, USA) with the dimension of 11mm × 4 mm. Inlet and outlet were cut on a Poly(methyl methacrylate) (PMMA) sheet with 3 mm diameter. To cut the PMMA following parameters were set: scan speed of 6 mm/s, power of 83W, pulse per inch rate of 500, and 0.125 inches for laser height. The DSA was peeled off and attached on top of the electrodes that were microfabricated on a glass substrate. The other side of the DSA was then attached to the PMMA with inlet and outlet (Shafiee et al. 2013).

Electric Field Simulation

The electrical field and its gradient $\nabla E = \nabla(\nabla\varphi)$ were modeled using AC/DC module of COMSOL Multiphysics 3.5a (Burlington, MA, USA), where Φ is the potential distribution. The governing equation to solve for gradient electric field intensity was $\nabla.(\sigma^*\nabla(\varphi)) = 0$, where σ* is the complex conductivity of the various sub-domains. Boundary conditions are set as follows: the voltages of each side of electrodes are set to arbitrary values and 0, respectively. The conductivities of gold electrode and DEP buffer were 1 S/cm and 100 μS/cm, respectively. The relative permittivity of gold and DEP buffer was set at 1 and 2.65, respectively.

Viability assay

On-chip cell viability was tested DEP buffer I. A 10 μl aliquot of cells suspended in DEP buffer and incubated for 15 minutes was mixed with 30 μl of Trypan Blue. A 10 μl aliquot of the cell-Trypan blue mixture was then counted using a haemocytometer.

Results and Discussion

Effect of frequency on the electrical response of latently infected B cells

Since the KSHV-infected BJAB cells constitutively express GFP, we first assessed how GFP expression might affect the electrical response of BJAB cells. Electrical response of BJAB and GFP-expressing BJAB cells were measured for different frequencies, flow rates, and applied voltages. As shown in Fig. S1, we did not observe any significant difference in cell capture efficiencies for BJAB and BJAB GFP cells at all applied frequencies, voltages, and sample flow rates ($n=3$, $p>0.05$). These results indicate that any cell electrical response difference between BJAB and latently KSHV-infected BJAB cells is independent of GFP expression. We then measured the electrical response of BJAB and KSHV-infected BJAB cells. Fluorescent imaging of KSHV infected BJAB cells and uninfected BJAB cells (Fig. 1C–H). Fig. 1C&D show the nuclei of uninfected and infected B cells. KSHV infected cells express the viral protein LANA, which concentrates to dots in cell nuclei, as previously described (Fig. 1F). Uninfected BJAB cells lack LANA (Fig. 1E). KSHV infected cells also express GFP from an expression cassette within the recombinant virus (Fig. 1H). Uninfected BJAB cells lack GFP (Fig 1G). The cell staining using anti-LANA antibody is toxic and destructive to the cells. Therefore, sorting infected cells using an on-chip label-free electrical sensing method is promising and novel.

Fig. 2A shows the capture efficiency of BJAB and KSHV latently-infected BJAB cells at 50 KHz and 75 KHz signal frequencies. 77.8%± 2.2% and 84.5%± 2.9% of the latently infected B cells were captured at 50 KHz and 75 KHz, respectively. In contrast, 51.1%± 0.8% and 64.4% ±2.6% of uninfected BJAB cells were captured at 50 KHz and 75 KHz, respectively. We also evaluated the Δ(C.E.) in samples with mixture of latently infected and uninfected cells (50% v/v). The Δ(C.E.) for selectively enriching latently infected cells was 26.6% ±6.7% and 20.1% ±11.6% at 50 KHz and 75 KHz, respectively.

By increasing frequency from 50 KHZ to 75 KHZ, the cell capture efficiency of KSHV-infected BJAB cells increased. Alternatively, by increasing the flow rate the capture

efficiency of cells decreased (Fig. 2A&B). This may be due to the fact that hydrodynamic forces were dominating the dielectrophoretic forces, which prevented the BJAB cells to attach on the surface of electrodes while KSHV-infected cells with higher DEP responses were captured. Consequently the Δ(C.E.) increased (Fig. 2C&D). Upon increasing frequency from 50 KHz to 75 KHz, Δ(C.E.) decreased due to increasing the DEP forces enhance capturing of both infected and uninfected BJAB cells. As shown in Fig. 2D, Δ(C.E.) was 37.1%±8.5% and 28.8%± 11.7% at 50KHz and 75 KHz, respectively.

Effect of applied voltage on the electrical response of latently infected B cells

The cell capture efficiency at an applied voltage of 0.5 V, signal frequency of 50 KHz, and flow rate of 0.01 μl/min was negligible (Fig. 3A–D). The cell capture efficiency for latently KSHV-infected BJAB cells reduced to 62% by increasing the flow rates from 0.01 μl/min to 0.02 μl/min (Fig. 3A&B). Alternatively, increasing the applied voltage to 1V caused the cell capture efficiency of latently KSHV-infected BJAB cells to reach as high as 78%± 3.85% with Δ(C.E.) of 26.6%±6.7% (Fig. 3C). We also evaluated the cell capture efficiency and Δ(C.E.) at 75 KHz (Fig. 3E–H). We observed that Δ(C.E.) increased by 10.5% (from 26.6% ±6.5% to 37.1%±8.5%) and by 8.4% (from 20.1%±11.5% to 28.3%±11.7%) at 50 KHz and 75 KHz, respectively when sample flow rate increased from 0.01 μl/min to 0.02 μl/min (Fig. 3C&D&G&H). The cell capture efficiency in our microchips was maximum (approximately 100%) for electrical signals equal and higher than 1 V. The cell capture efficiency for voltages lower than 0.5 V was also negligible. In addition, applied voltages higher than 0.5 V would create high electric filed intensities that would significantly affect the cell viability of on-chip captured cells.

Effect of flow rate on the electrical response of latently infected B cells

Sample flow rate can also have a significant effect on cell capture efficiency and Δ(C.E.). We evaluated the DEP response of the infected and uninfected BJAB cells for different sample flow rates. We observed that by increasing flow rate; capture efficiency of infected and uninfected cells decreased, due to increasing the hydrodynamic force (Fig. 4A&B&E). However, at 100 KHz frequency with different flow rates, we observed that capturing efficiencies reached to the maximum value and did not change significantly. This is due to the fact that DEP force at 100 KHz dominated the hydrodynamic force. Alternatively, increasing flow rate at 0.5 V applied voltage and frequencies of 75 KHz and 100 KHz, decreased Δ(C.E.) (Fig. 4C&D). Increasing flow rate at 1V and 75 KHz increased Δ(C.E.) to the value of 37% (Fig. 4G). Conversely, at 100 KHz and 1V, increasing the flow rate did not significantly change Δ(C.E.) (Fig. 4H). This is due to the fact that at 100 KHz almost all the infected and uninfected cells were captured on electrodes, which prevented proper cell separation. In this work, we conducted the experiments with flow rates below 0.04 μl/min as we did not observe any significant cell capture for flow rates higher than 0.04 μl/min.

Cell Viability

We evaluated cell viability in our DEP buffers as well as after on-chip cell capturing (Fig. 5). These results showed that more than 30 minutes incubation time in DEP buffer would have significant affect on cell viability of captured cells. Therefore, our on-chip sample processing time was less than 30 minutes. Our cell viability evaluation showed 75%

viability of both infected and uninfected BJAB cells in DEP buffer I for 30 minutes incubation time (Fig. 5A&D). For DEP buffers II and III, cell viability of infected and uninfected B cells was lower compared to DEP buffer I, during the first 30-minute of incubation (Fig. 5B&C&E&F). For uninfected cells BJAB, cell viability percentages for 30-minute incubation time in DEP buffer I, II, and III were 75%, 70% and 5%, respectively. The cell viabilities for KSHV-infected BJAB cells suspended in DEP buffers I, II, and III after 30 minutes incubation were 75%, 28% and 65%, respectively. Therefore, we chose DEP buffer I for our on-chip cell capture experiments. We also evaluated the effect of DEP on cell viability while capturing cells within 15 minutes on-chip incubation. We achieved 55% cell viability after 15 minutes on-chip cell capture and incubation (Fig. 5G).

On-chip captured cells experienced relatively high electric field intensities during the DEP experiments for applied voltages higher than 1 V, which may cause irreversible electroporation. Irreversible electroporation is a phenomenon, in which permanent pores appear on the membrane of the cells due to high electric field intensity that causes cell death (Wang et al. 2007). The gradient of the electric intensity on the chip was numerically modelled (Fig. S2). The cell viability in our microchip may be affected by electric field intensity due to irreversible electroporation. Further work is required to enhance the cell viability in the presented method through design optimization.

Conclusion

In this work, we have investigated the DEP response of latently infected and uninfected BJAB cells. We observed significant differences in the DEP response of latently KSHV-infected BJAB cells compared to uninfected BJAB cells such that they can be isolated on-chip using their electrical signatures. We have shown that the electrical response of latently KSHV-infected B cells is different from that of uninfected cells; this difference is due to the presence of infecting KSHV in infected B cell lines. At the operational parameters of 1V, 50 KHz, and 0.02 μl/min flow rate we were able to effectively separate 37.1%±8.5% of latently infected BJAB cells from uninfected BJAB cells. Our cell viability studies showed that 55% of captured cells were alive after 15 minutes of DEP separation during the experimental process. Further electrode dimension optimisation is required in order to reduce the electric field intensity and increase the cell viability on-chip. This work is the first to demonstrate that latently infected cells and uninfected cells show significantly different electrical response in microfluidic devices. The difference in electrical response may be due to the presence of the multiple copies of the ~165 Kbp negatively charged KSHV DNA genomes in latently infected BJAB cells. It may also be due to KSHV proteins expressed as well as the modifications they drive in the cell. At this point, it is difficult to make a final conclusion as to the reasons behind such electrical response differences between the infected and uninfected cells and more investigation is certainly needed. Specifically identifying and sorting latently infected cells may potentially open a new avenue for investigating viral-infected cells and possibly for therapeutic effective therapies.

Supplementary Material

Refer to Web version on PubMed Central for supplementary material.

Acknowledgments

The authors would like to thank the supports received from the National Institute of Allergy and Infectious Diseases (NIAID), National Institute of Health (NIH) (F32AI102590, 1R01AI118502), Brigham and Women's Hospital (BWH), Harvard Medical School (HMS) through Bright Futures Prize and Innovation Evergreen Fund, The National Science and Engineering Research Council of Canada (NSERC) through a postdoctoral fellowship, and Programme de Bourse pour de Court Séjours a l'étranger (PBCSE). This work is also supported in part by grants NIH NCI CA082036 and NIH NIDCR DE025208 (to KMK).

References

Aceti A, Bonincontro A, Cametti C, Celestino D, Leri O. Electrical conductivity of human erythrocytes infected with Plasmodium falciparum and its modification following quinine therapy. Trans R Soc Trop Med Hyg. 1990; 84(5):671–672. [PubMed: 2278066]

Archer S, Morgan H, Rixon FJ. Electrorotation studies of baby hamster kidney fibroblasts infected with herpes simplex virus type 1. Biophys J. 1999; 76(5):2833–2842. [PubMed: 10233099]

Becker FF, Wang XB, Huang Y, Pethig R, Vykoukal J, Gascoyne PR. Separation of human breast cancer cells from blood by differential dielectric affinity. Proc Nat Acad Sci USA. 1995; 92:860–864. [PubMed: 7846067]

Chen L, Lagunoff M. Establishment and maintenance of Kaposi's sarcoma-associated herpesvirus latency in B cells. J Virol. 2005; 79(22):14383–14391. [PubMed: 16254372]

Chun TW, Carruth L, Finzi D, Shen X, DiGiuseppe JA, Taylor H, Hermankova M, Chadwick K, Margolick J, Quinn TC, Kuo YH, Brookmeyer R, Zeiger MA, Barditch-Crovo P, Siliciano RF. Quantification of latent tissue reservoirs and total body viral load in HIV-1 infection. Nature. 1997; 387(6629):183–188. [PubMed: 9144289]

Chun TW, Finzi D, Margolick J, Chadwick K, Schwartz D, Siliciano RF. In vivo fate of HIV-1-infected T cells: quantitative analysis of the transition to stable latency. Nat Med. 1995; 1(12):1284–1290. [PubMed: 7489410]

Donthu S, Zixiao Pan Z, Myers B, Shekhawat B, Wu N, Dravid V. Facile scheme for fabricating solid-state nanostructures using e-beam lithography and solution precursors. Nano Lett. 2005; 5(9):1710–1715. [PubMed: 16159210]

Finzi D, Blankson J, Siliciano JD, Margolick JB, Chadwick K, Pierson T, Smith K, Lisziewicz J, Lori F, Flexner C, Quinn TC, Chaisson RE, Rosenberg E, Walker B, Gange S, Gallant J, Siliciano RF. Latent infection of CD4+ T cells provides a mechanism for lifelong persistence of HIV-1, even in patients on effective combination therapy. Nature Med. 1999; 5:512–517. [PubMed: 10229227]

Finzi D, Hermankova M, Pierson T, Carruth LM, Buck C, Chaisson RE, Quinn TC, Chadwick K, Margolick J, Brookmeyer R, Gallant J, Markowitz M, Ho DD, Richman DD, Siliciano RF. Identification of a reservoir for HIV-1 in patients on highly active antiretroviral therapy. Science. 1997; 278(5341):1295–1300. [PubMed: 9360927]

Ganem D. KSHV infection and the pathogenesis of Kaposi's sarcoma. Annu Rev Pathol. 2006; 1:273–296. [PubMed: 18039116]

Ganem, D. Kaposi's sarcoma-associated herpesvirus. In: Knipp, DM.; Howley, P., editors. Field virology. Lippincott Wiliams & Wilkins; Philadelphia, PA: 2007. p. 2847-2888.

Gascoyne P, Pethig R, Satayavivad J, Becker FF, Ruchirawat M. Dielectrophoretic detection of changes in erythrocyte membranes following malarial infection. Biochim Biophys Acta. 1997; 1323(2):240–252. [PubMed: 9042346]

Guo Q, Reiling SJ, Rohrbach P, Ma H. Microfluidic biomechanical assay for red blood cells parasitized by Plasmodium falciparum. Lab Chip. 2012; 12:1143–1150. [PubMed: 22318405]

Hamden KE, Bryan BA, Ford PW, Xie C, Li YQ, Akula SM. Spectroscopic analysis of Kaposi's sarcoma-associated herpesvirus infected cells by Raman tweezers. J Virolog Meth. 2005; 129:145–151.

Hampl H, Schlehofer JR, Habermehl KO. Differences in the morphology of herpes simplex virus infected cells. II. Type specific membrane alterations of HSV-1 and HSV-2 infected cells. Med Microbiol Immunol. 1981; 169(3):209–223. [PubMed: 6265748]

Jokerst, NM.; Brooke, MA.; Allen, MG. Processes for lift-off of thin film materials or devices for fabricating three dimensional integrated circuits, optical detectors, and micromechanical devices. 1995. WO1993021663A1, US

Jones D, Ballestas ME, Kaye KM, Gulizia JM, Winters GL, Fletcher J, Scadden DT, Aster JC. Primary-effusion lymphoma and Kaposi's sarcoma in a cardiac-transplant recipient. New Engl J Med. 1998; 339:444–449. [PubMed: 9700178]

Kikuta H, Itakura O, Taneichi K, Kohno M. Tropism of human herpesvirus 8 for peripheral blood lymphocytes in patients with Castleman's disease. Brit J Haematol. 1997; 99:790–793. [PubMed: 9432023]

Krempien U, Jockusch BM, Jungwirth C. Herpes simplex virus-induced cell surface protrusions. Intervirology. 1984; 22(3):156–163. [PubMed: 6500889]

Moor K, Ohtani K, Myrzakozha D, Zhanserkenova O, Andriana B, Sato H. Noninvasive and label-free determination of virus infected cells by Raman spectroscopy. J Biomed Opt. 2014; 19(6):067003. [PubMed: 24898605]

Nam J, Huang H, Lim H, Lim C, Shin S. Magnetic Separation of Malaria-Infected Red Blood Cells in Various Developmental Stages. Anal Chem. 2013; 85(15):7316–7323. [PubMed: 23815099]

Pohl H, Crane J. Dielectrophoresis of Cells. Biophys J. 1971; 11(9):711–727. [PubMed: 5132497]

Rixon FJ, Addison C, McLauchlan J. Assembly of enveloped tegument structures (L particles) can occur independently of virion maturation in herpes simplex virus type 1-infected cells. J Gen Virol. 1992; 73(Pt 2):277–284. [PubMed: 1311357]

Salmanzadeh A, Romero L, Shafiee H, Gallo-Villanueva RC, Stremler MA, Cramer SD, Davalos RV. Isolation of prostate tumor initiating cells (TICs) through their dielectrophoretic signature. Lab Chip. 2012a; 12(1):182–189. [PubMed: 22068834]

Salmanzadeh A, Sano MB, Shafiee H, Stremler MA, Davalos RV. Isolation of rare cancer cells from blood cells using dielectrophoresis. IEEE Eng Med Biol Soc. 2012b; 2012:590–593.

Schlehofer JR, Hampl H, Habermehl KO. Differences in the morphology of herpes simplex virus infected cells: I. Comparative scanning and transmission electron microscopic studies on HSV-1 infected HEp-2 and chick embryo fibroblast cells. J Gen Virol. 1979; 44(2):433–442. [PubMed: 230292]

Shafiee H, Caldwell JL, Sano MB, Davalos RV. Contactless dielectrophoresis: a new technique for cell manipulation. Biomed Microdevices. 2009; 11:997–1006. [PubMed: 19415498]

Shafiee H, Jahangir M, Inci F, Wang S, Willenbrecht R, Giguel FF, Tsibris A, Kuritzkes DR, Demirci U. Acute On-Chip HIV Detection Through Label-Free Electrical Sensing of Viral Nano-Lysate. Small. 2013; 9(15):2553–2563. [PubMed: 23447456]

Shafiee H, Sano MB, Henslee EA, Caldwell JL, Davalos RV. Selective isolation of live/dead cells using contactless dielectrophoresis (cDEP). Lab Chip. 2010; 10(4):438–445. [PubMed: 20126683]

Soo Hoo W, Wang M, Kohrumel J, Hall J. A novel method for detection of virus-infected cells through moving optical gradient fields using adenovirus as a model system. Cytometry A. 2004; 58(2):140–146. [PubMed: 15057967]

Soulier J, et al. Kaposi's sarcoma-associated herpesvirus-like DNA sequences in multicentric Castleman's disease. Blood. 1995; 86:1276–1280. [PubMed: 7632932]

Tseng AA, C K, Chen CD, Ma KJ. Electron beam lithography in nanoscale fabrication: recent development. IEEE Trans Electron Pack Manuf. 2003:141–149.

Vieu C, Carcenac F, Pepin A, Chen Y, Mejias M, Lebib A, Manin-Ferlazzo L, Couraud L, Launois H. Electron beam lithography: resolution limits and applications. Appl Surf Sci. 2000; 164:111–117.

Villarreal, LP. Viruses and the evolution of life. Asm Press; Washington: 2005.

Wang H, Banada P, Bhunia A, Lu C. Rapid electrical lysis of bacterial cells in a microfluidic device. Methods Mol Biol. 2007; 385:23–35. [PubMed: 18365702]

Wong JK, Hezareh M, Gunthard HF, Havlir DV, Ignacio CC, Spina CA, Richman DD. Recovery of replication-competent HIV despite prolonged suppression of plasma viremia. Science. 1997; 278(5341):1291–1295. [PubMed: 9360926]

Highlights

- Dielectrophoresis (DEP) response of latently KSHV-infected BJAB cells were investigated and compared with the DEP response of uninfected BJAB cells.
- The cell capture efficiency of uninfected and KSHV-infected BJAB cells were investigated using a DEP-based microfluidic device with interdigitated electrodes.
- The difference between cell capture efficiencies for uninfected and KSHV-infected BJAB cells was 37.1%%±8.5%.

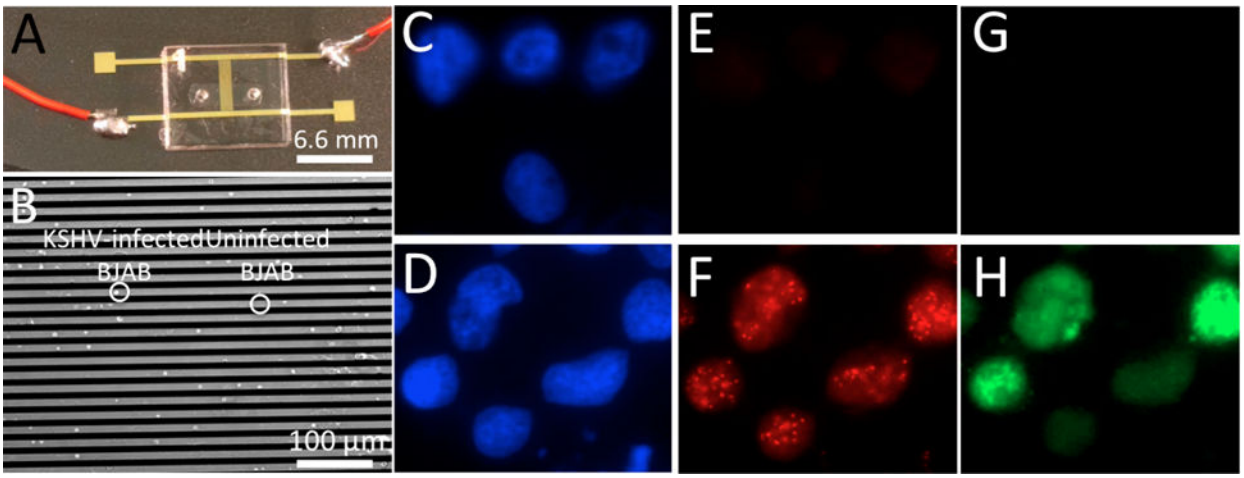

Fig. 1.

DEP microchip platform to evaluate the electrical response of KSHV-infected and uninfected BJAB cells. (A) Image of the DEP microchip. (B) Microscopy image of captured KSHV-infected and uninfected BJAB cells. Uninfected (C, E, G) and KSHV-infected (D, F,H) BJAB cells. (C,D) Nuclei were detected by counterstaining DNA with Hoechst 33258 (blue). (E, G) Uninfected BJAB cells lack LANA and do not express GFP. (F) KSHV-infected BJAB cells express the viral protein LANA (red) which concentrates to dots at sites of KSHV genomes. (H) These cells also express GFP (green) from an expression cassette within the recombinant virus.

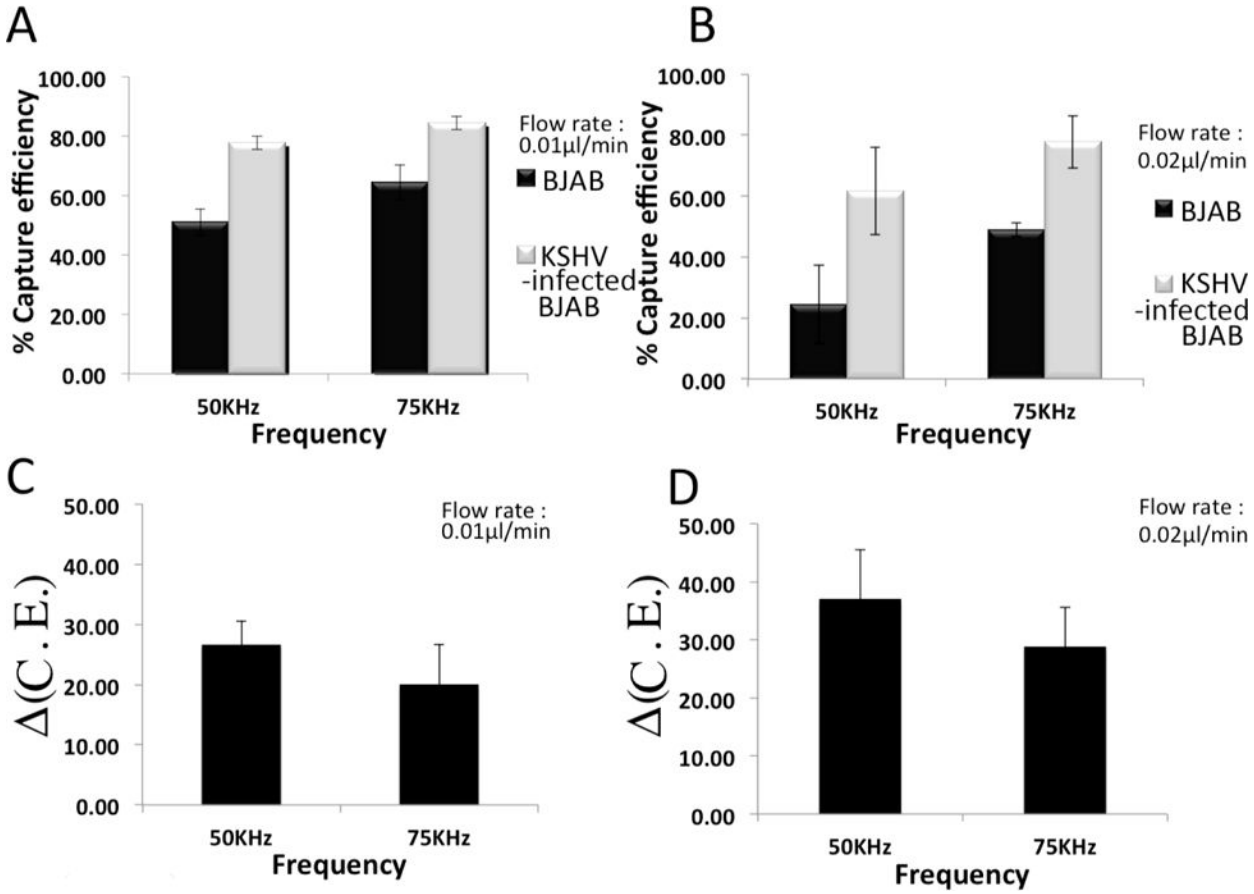

Fig. 2.

Capture efficiencies of BJAB and latently KSHV-infected BJAB cells for various frequencies at constant flow rates of (A) 0.01 µl/min and (B) 0.02 µl/min. Δ(*C*. E.) at various frequencies with flow rates of (C) 0.01 µl/min and (D) 0.02 µl/min. The applied potential was kept constant at 1V. Experiments were repeated 3 times (n=3).

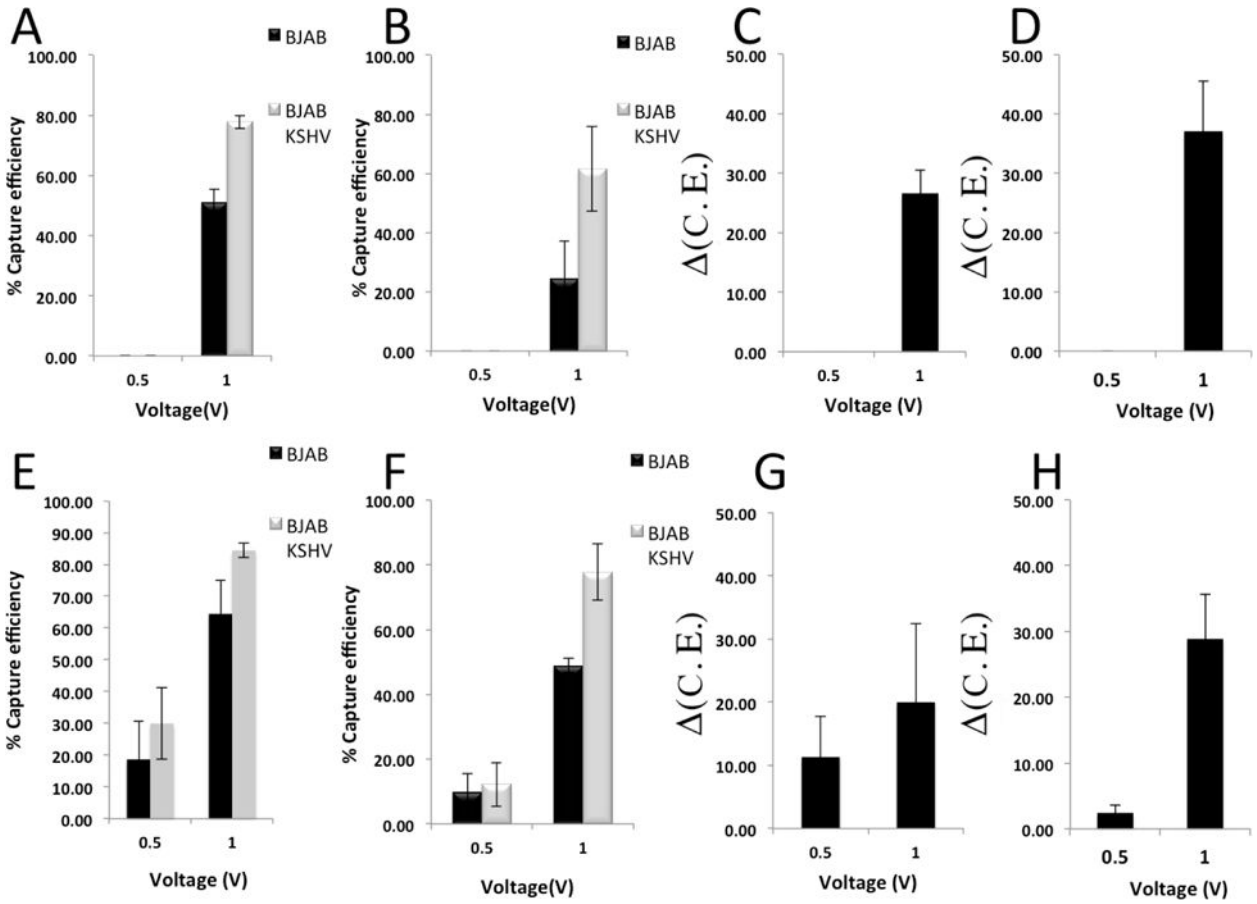

Fig. 3.

Capture efficiency and Δ(C.E.) for different applied voltages at constant flow rates and frequencies. (A–D) The frequencies were set to 50 KHz. Capture efficiency of uninfected and KSHV-infected BJAB cells for different applied voltages at flow rates of (A) 0.01 μl/min and (B) 0.02 μl/min. Δ(C.E.) at flow rates of (C) 0.01 μl/min and (D) 0.02 μl/min. (E–H) The frequencies were set to 75 KHz. Capture efficiency of uninfected and KSHV-infected BJAB cells for different applied voltages at flow rates of (E) 0.01 μl/min and (F) 0.02 μl/min. Δ(C.E.) at flow rates of (G) 0.01 μl/min and (H) 0.02 μl/min. Experiments were repeated 3 times (n=3).

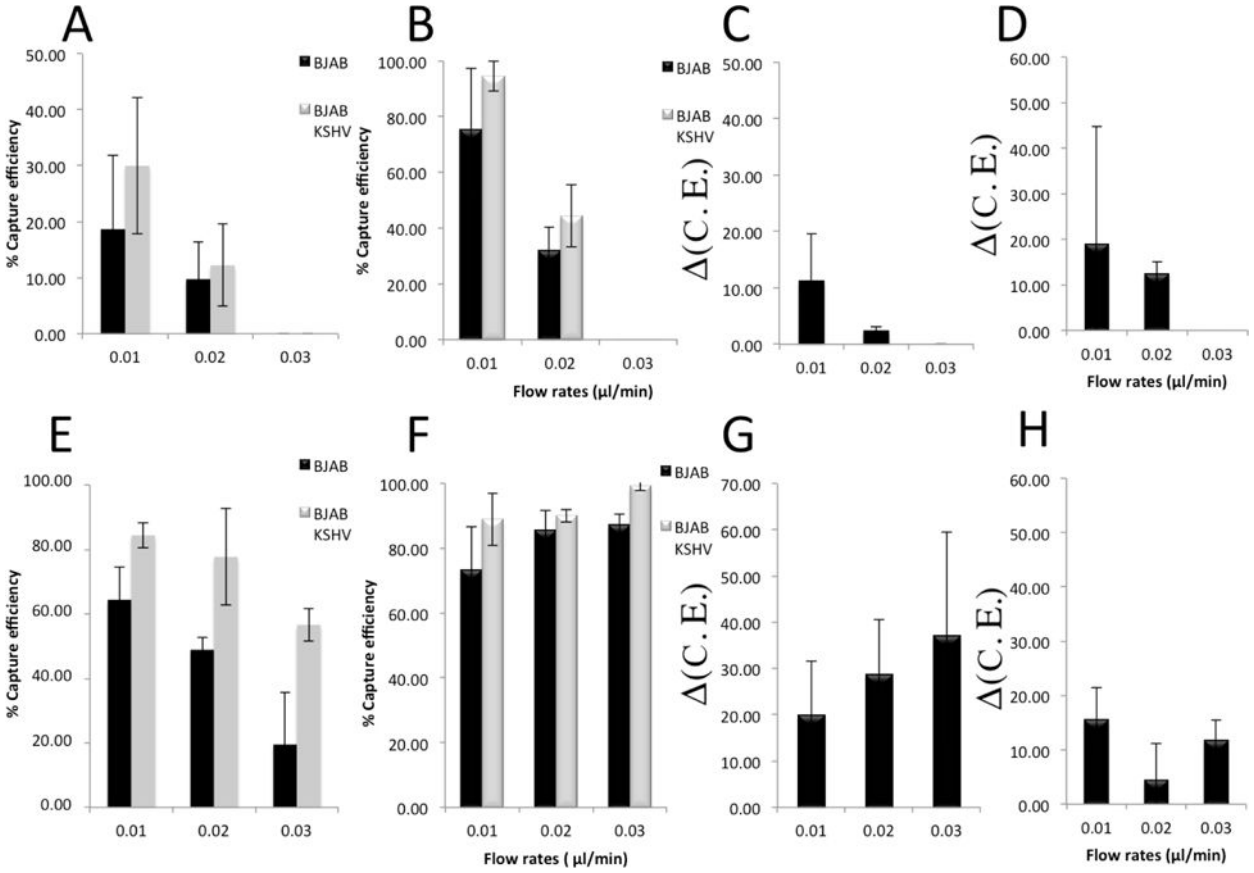

Fig. 4.

Capture efficiency and Δ(C.E.) for different flow rates at constant applied potential and frequencies. (A–D) The applied potential were set to 0.5 V. Cell capture efficiency of BJAB and KSHV-infected BJAB cells for different flow rates at frequencies of (A) 75 KHz and (B) 100 KHz. Δ(C.E.) of KSHV-infected BJAB cells at frequencies of (C) 75 KHz and (D) 100 KHz. (E–F) The applied potential were set to 1 V. Capturing efficiency of BJAB and KSHV-infected BJAB cells for different flow rates at frequencies of (E) 75 KHz and (F) 100 KHz. Δ(C.E.) at frequencies of (G) 75 KHz, (H) 100 KHz. Experiments were repeated 3 times (n=3).

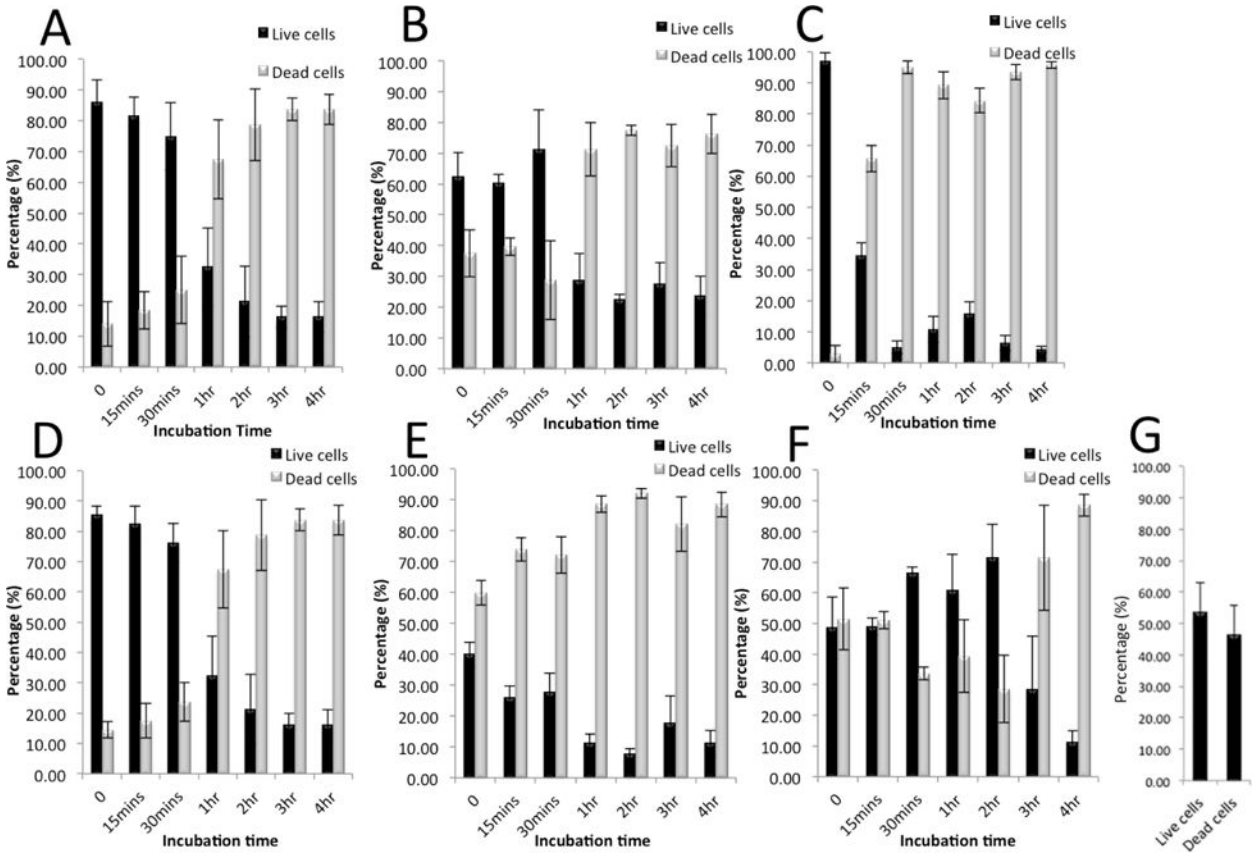

Fig. 5.

Cell viability analysis of BAJB and KSHV-infected BJAB cells before and after injecting into the DEP microfluidic chip in various DEP media for different incubation times over a period of 4 hours. Percentage of live/dead (A) BJAB cells in DEP Buffer I, (B) BJAB cells in DEP Buffer II, (C) BJAB cells in DEP Buffer III, (D) KSHV-infected BJAB cells in DEP Buffer I, (E) KSHV-infected BJAB cells in DEP Buffer II, and (F) KSHV-infected BJAB cells in DEP Buffer III. (G) The percentage of live/dead cells after on-chip cell capture.